

# $^1\text{H}$ qNMR-Based Metabolomics Discrimination of Covid-19 Severity

Banny S. B. Correia, Vinicius G. Ferreira, Priscila M. F. D. Piagge, Mariana B. Almeida, Nilson A. Assunção, Joyce R. S. Raimundo, Fernando L. A. Fonseca, Emanuel Carrilho, and Daniel R. Cardoso\*



Cite This: <https://doi.org/10.1021/acs.jproteome.1c00977>



Read Online

ACCESS |



Metrics & More



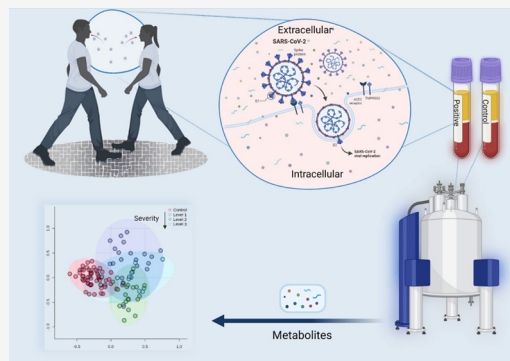
Article Recommendations



Supporting Information

**ABSTRACT:** The coronavirus disease 2019 (Covid-19), which caused respiratory problems in many patients worldwide, led to more than 5 million deaths by the end of 2021. Experienced symptoms vary from mild to severe illness. Understanding the infection severity to reach a better prognosis could be useful to the clinics, and one study area to fulfill one piece of this biological puzzle is metabolomics. The metabolite profile and/or levels being monitored can help predict phenotype properties. Therefore, this study evaluated plasma metabolomes of 110 individual samples, 57 from control patients and 53 from recent positive cases of Covid-19 (IgM 98% reagent), representing mild to severe symptoms, before any clinical intervention. Polar metabolites from plasma samples were analyzed by quantitative  $^1\text{H}$  NMR. Glycerol, 3-aminoisobutyrate, formate, and glucuronate levels showed alterations in Covid-19 patients compared to those in the control group (Tukey's HSD  $p$ -value cutoff = 0.05), affecting the lactate, phenylalanine, tyrosine, and tryptophan biosynthesis and D-glutamine, D-glutamate, and glycerolipid metabolisms. These metabolic alterations show that SARS-CoV-2 infection led to disturbance in the energetic system, supporting the viral replication and corroborating with the severe clinical conditions of patients. Six polar metabolites (glycerol, acetate, 3-aminoisobutyrate, formate, glucuronate, and lactate) were revealed by PLS-DA and predicted by ROC curves and ANOVA to be potential prognostic metabolite panels for Covid-19 and considered clinically relevant for predicting infection severity due to their straight roles in the lipid and energy metabolism. Thus, metabolomics from samples of Covid-19 patients is a powerful tool for a better understanding of the disease mechanism of action and metabolic consequences of the infection in the human body and may corroborate allowing clinicians to intervene quickly according to the needs of Covid-19 patients.

**KEYWORDS:** Covid-19, metabolomics, NMR, prognosis



## INTRODUCTION

With an estimated cost of more than 6.3 million deaths and trillions of dollars in the worldwide economic breakdown, the coronavirus disease 2019 (Covid-19) has impacted the lives of the entire globe.<sup>1,2</sup> The economic and social consequences of the Covid-19 pandemic will last for many years; however, it also reshaped science and caused a race for scientific evolution in many areas.<sup>3</sup> The entire world joined forces, resources, and knowledge to fight the virus, from health-care workers to pharmaceutical companies and research institutes. As a result, several tests, health protocols, and vaccines arrived on the market, quickly as possible, resulting in the downfall of Covid-19 cases. Since the World Health Organization (WHO) received an alert about an unknown disease in China, 27 months passed, accumulating more than 530 million confirmed cases, 11.8 billion vaccine doses distributed, and more than 180,000 papers published on the topic.<sup>1</sup>

However, the risk of critical mutations remains active and concerns the scientific community, particularly for mutations in the spike protein responsible for the virus entry in human

cells through the ACE2 receptor and one of the main targets of immunologic response.<sup>4,5</sup> Mutations in the spike protein may generate higher transmissivity and even immunologic response evasion, decreasing the vaccination efficacy and threatening new outbreaks. Currently, the Center for Disease Control and Prevention (CDC) considers variants to be monitored, the Alpha, Beta, Gamma, Delta, Epsilon, Eta, Iota, Kappa, B.1.617.3, Mu, and Zeta, and variants of concern, Delta and Omicron.<sup>6,7</sup>

The disease, in general, causes severe respiratory problems, and its main symptoms are fever, fatigue, and cough.<sup>8</sup> Symptoms range from mild to severe, and about 80% of people recover from the disease without requiring hospital

**Received:** December 27, 2021

treatment.<sup>9</sup> However, 20% develop respiratory failure and dysfunction of other organs requiring urgent oxygen therapy or specific interventions.<sup>9,10</sup> It is noteworthy that the risk of death within 12 months following severe Covid-19 infection increases more than 200% compared to uninfected or mild symptom patients.<sup>11</sup> Notwithstanding, besides the elderly and those with comorbidities such as high blood pressure, heart and lung problems, diabetes, or cancer presenting a higher risk of becoming seriously ill,<sup>12–14</sup> people without known comorbidities with Covid-19 may also develop a severe case or a postacute Covid-19 syndrome (PACS), a condition characterized by long-term complications after Covid-19 infection, such as chest pain, fatigue, metabolic disruption, neurological sequelae, and thromboembolic conditions.<sup>15–19</sup> In fact, PACS is currently one primary concern for clinicians due to its impact on the patients' quality of life<sup>20</sup> and even on the world economy since affected patients are unable to perform their occupations normally.<sup>15,20</sup>

The physiological and metabolic changes associated with the disease are still not perfectly understood. In this way, it is essential to understand better the molecular pathways involved in the progression of severe Covid-19, which will provide more targeted treatments and strategies.<sup>8,21,22</sup> Previous studies have demonstrated dramatic alterations of the metabolome and lipidome in human plasma caused by various diseases, including infections by SARS-CoV-2, where intracellular parasites compete for the host cell nutrients and metabolites leading to alteration of the host metabolome.<sup>23–25</sup>

Studies are still required regarding biological markers that might help in fast and easy diagnosis and, most importantly, in the prognosis of patient's predisposition of severe Covid-19 symptoms, not only for new daily cases but also as preparation for possible new outbreaks. Within this context, the present work aims to perform <sup>1</sup>H NMR-based metabolomics in plasma samples collected from healthy controls (negative) and Covid-19 patients before any medical or drug treatment. All of the sample donors were included in the data analysis, even in the case of fatalities and recovery from mild to severe symptoms, to evaluate whether the metabolic panel might indicate this clinical distinction through multivariate statistical analysis.

## MATERIALS AND METHODS

### Samples

Blood samples from Covid-19 infected patients were collected in EDTA tubes at the moment of admission to the hospital, while healthy control samples were collected from health-care workers from the hospital. The blood samples were aliquoted for clinical tests, and patients were further submitted to RT-PCR (swab nasopharyngeal and oral) and antibody tests (plasma IgM) for SARS-Cov-2 virus infection confirmation. Aliquots of the blood samples were centrifuged at 1000g for 10 min at 25 °C for plasma separation. Plasma samples were then stored in a –80 °C freezer. A total of 110 samples were collected and analyzed, 57 being control samples (negative) and 53 being positive samples of Covid-19, 21 being from mild symptom patients (level 1), 22 from moderate symptom patients (level 2), and 10 from severe symptom patients (level 3). Mild symptoms were considered: fever, fatigue, cough, runny nose, and sneezing, with normal pulmonary examinations. Moderate cases were considered, where patients reported clinical signs of pneumonia, persistent fever, and low blood oxygen saturation. Severe cases were considered,

where the patients reported signs of pneumonia and severe respiratory distress and required intensive-care-unit admission. This study protocol was approved by the Ethics Committee of Universidade Federal de São Paulo, CAAE no. 43260121.1.1001.5505.

### Plasma Metabolite Extraction

Before viral inactivation, all plasma samples were handled in level 2 biosafety cabinets. The metabolites from plasma samples were extracted and inactivated by adding methanol in a 1:4 (plasma/methanol, v/v) proportion, which promotes protein precipitation and viral inactivation in a straightforward step.<sup>26</sup> After protein precipitation, samples were centrifuged at 10,000g for 10 min at 4 °C, and the supernatants were dried at speedvac (Speedvac<sup>R</sup> Concentrator SPD131DDA-115, Thermo Fischer) and stored at –80 °C until analysis.

The dried extracts containing the polar metabolites were resuspended in 750 μL of a deuterium oxide phosphate buffer (0.10 M, pD = 7.1) containing 0.7 mM of deuterated sodium trimethylsilylpropanesulfonate (DSS-*D*<sub>6</sub>) and 0.02% w/w of sodium azide. Then, they were filtered in 0.22 μm Teflon membranes and 550 μL was transferred to a 5 mm NMR tube for analysis.

### NMR Analysis

NMR spectra were conducted at 298 K on a 500 MHz (11.7 T) Agilent DD2 spectrometer with a 5 mm OneNMR probe with gradient capability. The spectra were acquired for proton NMR using the presaturation pulse sequence (Agilent PRESAT pulse sequence) for the water suppression, 32 K data points, with a spectral width of 16.0306 ppm, an acquisition time of 4.089 s, a fixed receiver gain of 46, a recycle delay of 41 s (5\*T<sub>1</sub>), dummy scans of 2, and an accumulation of 128 transients.

FIDs were multiplied by a 0.3 Hz exponential multiplication function prior to the Fourier transform. Phase and baseline corrections were carried out within instrument software, and the reference standard (DSS-*d*<sub>6</sub>) signal was calibrated at δ 0.00 ppm. The one-dimensional (1D) spectra were assigned using Chenomx NMR Suite software as a database supported by the literature and the two-dimensional (2D) NMR spectra (gCOSY, gHSQC) were obtained for selected samples, and spectral annotations were further analyzed using the COLMARM web server (<http://spin.ccic.osu.edu/index.php/colmarm/index/>) for (semi-) automated profiling. Metabolite peaks were integrated and quantified relative to DSS-*D*<sub>6</sub> 0.7 mM using Chenomx software for quantification.

### Statistical Analysis

Metabolite concentrations were analyzed in the MetaboAnalyst 5.0 platform (<http://www.metaboanalyst.ca/faces/home.xhtml>) using principal component analysis (PCA) and partial least-squares discriminant analysis (PLS-DA). Data preprocessing involved no data filtering, sample normalization by the median, data transformation by log transformation, and mean centering scaling (mean-centered only). Five principal components were used for the discrimination of the analyzed metabolite samples. Specifically, for PLS-DA, we applied leave-one-out cross-validation (LOOCV) as the cross-validation method. The accuracy and variable importance in projection (VIP) were also assessed to measure the performance and importance features of the analysis, respectively. For binary data comparisons, the receiver operating characteristic (ROC) curve was also applied for model validation, and probability

**Table 1. Demographic Information of Sample Groups<sup>b</sup>**

sample groups	age (Mean ± SD)	males (%)	females (%)	IgM <sup>a</sup> (%)	IgG <sup>a</sup> (%)	
control (n = 57)	42 ± 19	44	58	0	0	
Covid-19	level 1 (n = 21)	46 ± 15	57	43	100	62
	level 2 (n = 22)	57 ± 17	55	45	100	86
	level 3 (n = 10)	59 ± 11	60	40	90	50

<sup>a</sup>Data were obtained from the patient's chart. <sup>b</sup>SD: standard deviation.

**Table 2. <sup>1</sup>H NMR Assignments of Major Metabolites from Plasma Samples**

metabolites	NMR peak assignment
3-aminoisobutyrate	1.18 (d; 3H), 2.59 (m; 1H), 3.02 (dd; 1H), 3.10 (dd; 1H)
acetate	1.91 (s; 3H)
alanine	1.47 (d; 3H), 3.78 (q; 1H)
citrate	2.52 (d; 2H), 2.68 (d; 2H)
creatine	3.03 (s; 3H), 3.91 (s; 2H)
formate	8.45 (s; 1H)
glucose	3.25 (m; 1H), 3.41 (m; 2H), 3.48 (m; 2H), 3.54 (dd; 1H), 3.72 (m; 3H), 3.76 (dd), 3.82 (m; 2H), 3.89 (dd; 1H), 4.65 (d; 1H), 5.23 (d; 1H)
glucuronate	3.27 (m; 1H), 3.49 (m; 2H), 3.57 (dd; 1H), 3.71 (m; 1H), 4.05 (d; 1H), 4.65 (d; 2H), 5.23 (d; 1H)
glutamate	2.04 (m; 2H), 2.13 (m; 2H), 3.35 (m; 1H), 3.75 (m)
glycerol	3.55 (m; 4H), 3.64 (m; 4H), 3.78 (m; 1H)
lactate	1.32 (d; 3H), 4.10 (q; 1H)
leucine	0.94 (d; 3H), 0.96 (d; 3H), 1.71 (m; 3H); 3.73 (dd; 1H)
phenylalanine	3.12 (m; 1H), 3.28 (m; 1H), 3.99 (dd; 2H), 7.32 (d; 2H), 7.40 (t; 1H), 7.42 (t; 2H)
pyruvate	2.37 (s; 3H)
threonine	1.32 (d; 3H), 3.58 (d; 1H), 4.25 (m; 1H)
tryptophan	7.19 (t; 1H), 7.28 (t; 1H), 7.32 (s; 1H), 7.54 (d; 1H), 7.73 (d; 1H)
tyrosine	6.88 (d; 2H), 7.18 (d; 2H)
valine	0.97 (d; 3H), 1.03 (d; 3H), 2.25 (m; 1H), 3.59 (d; 1H)

view graphs were generated from ROC curves to assess the prediction probability of the model.

For one-way analysis of variance (ANOVA), an adjusted *p*-value (FDR) cutoff of 0.05 was applied, and Tukey's honestly significant difference (Tukey's HSD) was used as post hoc analysis in GraphPad Prism 5.0 (La Jolla, CA, 2008) software. Pathway analysis was performed, applying the differential metabolites cross-listed with the pathways in the Kyoto Encyclopedia of Genes and Genomes (KEGG), using the previous identification at Kyoto Encyclopedia of Genes and Genomes (KEGG) of *Homo sapiens*, and the top altered pathways were identified and built according to the potential functional analysis. For this purpose also, the MetaboAnalyst 5.0 platform was employed.

## RESULTS

### Demographic Information

Table 1 summarizes the patients' demographic information. Controls and level 1 patient's (mild symptoms) age were similar, 42 ± 19 and 46 ± 15, respectively, while level 2 (moderate) and level 3 (severe) patients had an average age of 57 ± 17 and 59 ± 11, respectively. Therefore, as expected and widely reported, there was a correlation between the symptom's severity and patient's age.<sup>13,27–29</sup> From our sample group, a slight majority of the Covid-19 groups were males, approximately 57%. All patients within the Covid-19 group were tested for IgM and IgG, with 100% confirmation for IgM presence and approximately 66% for IgG incidence. Age and sex were not taken into account for the statistical model to search for general differences between Covid-19 levels.

### Covid-19 Positive vs Control Samples

One hundred and ten plasma samples were analyzed by <sup>1</sup>H qNMR analysis, followed by identification, multivariate statistical analysis, and interpretation, resulting in 18 potential discriminant metabolites. The metabolomic profile is described in Table 2 and Figure S1. The compound identification relied first on the Chenomix software library, with additional double-checking through 2D spectral data (Table S2). However, some compounds, such as glucose and glucuronate, were identified exclusively using the Chenomix software library since their 2D NMR spectra data showed overlapping signals, as shown in Figure S2.

The metabolite concentrations obtained for each sample were first compared regarding positive vs negative diagnostics of Covid-19, enlightening the metabolic differences caused by the disease.

The supervised PLS-DA multivariate analysis (Figure 1A) separated the positive from negative groups. The PLS-DA model validation can be accessed by cross-validation, with *R*<sup>2</sup> and *Q*<sup>2</sup> coefficient values of 0.73 and 0.67, respectively (Figure 1B). A permutation test was also performed along with cross-validation, applying the prediction during the training test and 2000 permutations, resulting in an empirical *p* < 0.0005 (Figure 1C). The ROC curve generated (Figure 1D) presented an area under the curve (AUC) of 0.924 (95% CI: 0.843–0.972), highlighting the capability of the model to predict the group to which the sample belongs, with a confusion matrix with eight misses from 110 samples (Figure 1E).

The most critical metabolites for positive vs negative group discrimination were glycerol, 3-aminoisobutyrate, and acetate, as reported in Figure 1F. For this cohort, glycerol and 3-aminoisobutyrate levels were lower in positive samples, while acetate, phenylalanine, leucine, and lactate levels were higher in

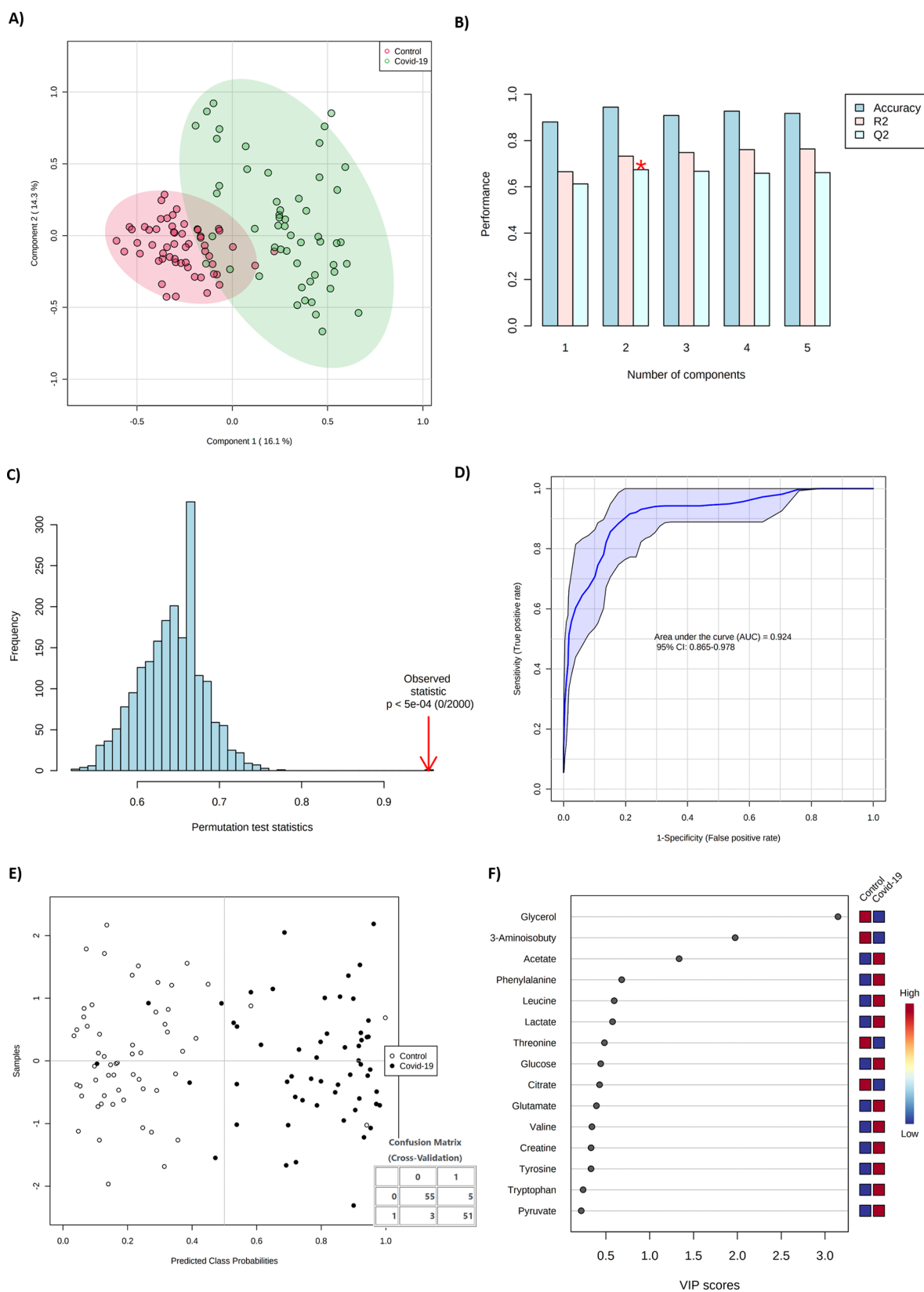


**Figure 1.** PLS-DA and cross-validation analysis of NMR metabolomics concentration data. (A) PLS-DA of Covid-19 samples vs health control, confidence interval = 95%; (B) cross-validation model from PLS-DA analysis, plotting  $R^2$ ,  $Q^2$ , and accuracy; (C) permutation test for the PLS-DA model validation,  $p < 0.0005$ ; (D) ROC curve for the predictive model, AUC = 0.924; (E) probability view for cross-validation; and (F) variable importance for the projection (VIP) scores.

Covid-19 positive samples (Figure 1F and Table S2). The metabolite panel for positive vs negative group classification as

obtained by binning the spectra data also corroborates with the qNMR results and is shown in Figure S3.

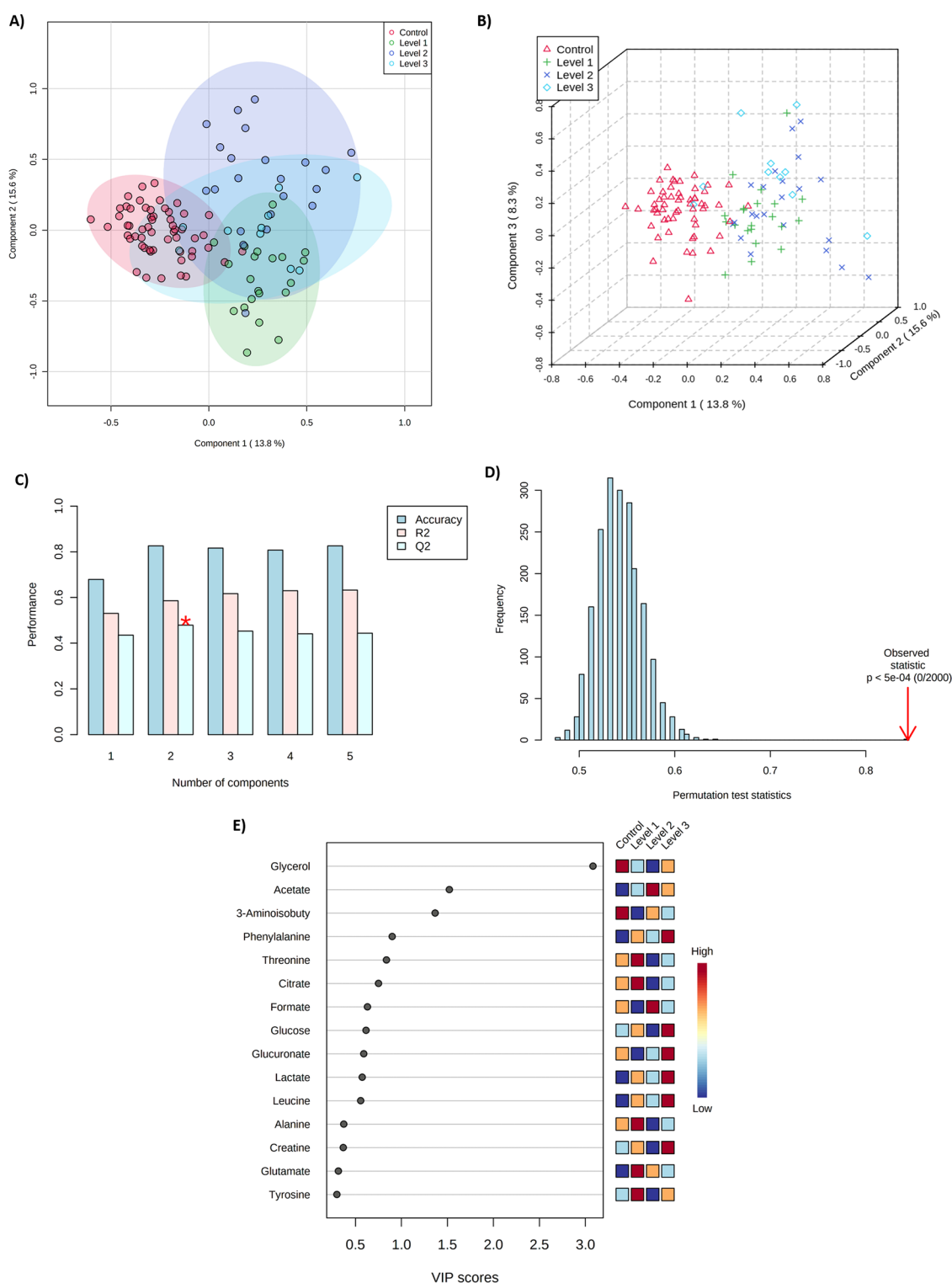


**Figure 2.** PLS-DA and cross-validation analysis of NMR metabolomics data accordingly with Covid-19 symptom severity. (A) PLS-DA model with a 95% confidence interval for each group; (B) PLS-DA projection in three dimensions; (C) cross-validation model of the analysis, plotting  $R^2$ ,  $Q^2$ , and accuracy; (D) permutation test for the generated model; and (E) variable importance for the projection scores.

### Disease Severity Panel of Metabolite as Potential Plasma Biomarkers

Another statistical data analysis approach was performed, comparing the control group *vs* the positive group by severities. These groups were previously categorized according to the patients' symptoms but, it is essential to notice that the severity status of the patients represents the conditions they underwent

after hospital admission, not the immediate severity at the sampling moment.

For severity group analysis, the samples were considered (i) control, (ii) level 1—mild symptoms, (iii) level 2—moderate symptoms, and (iv) level 3—severe symptoms. Similarly, with the prior comparison, PLS-DA multivariate analysis was able to show a tendency of discrimination (Figure 2A), although even



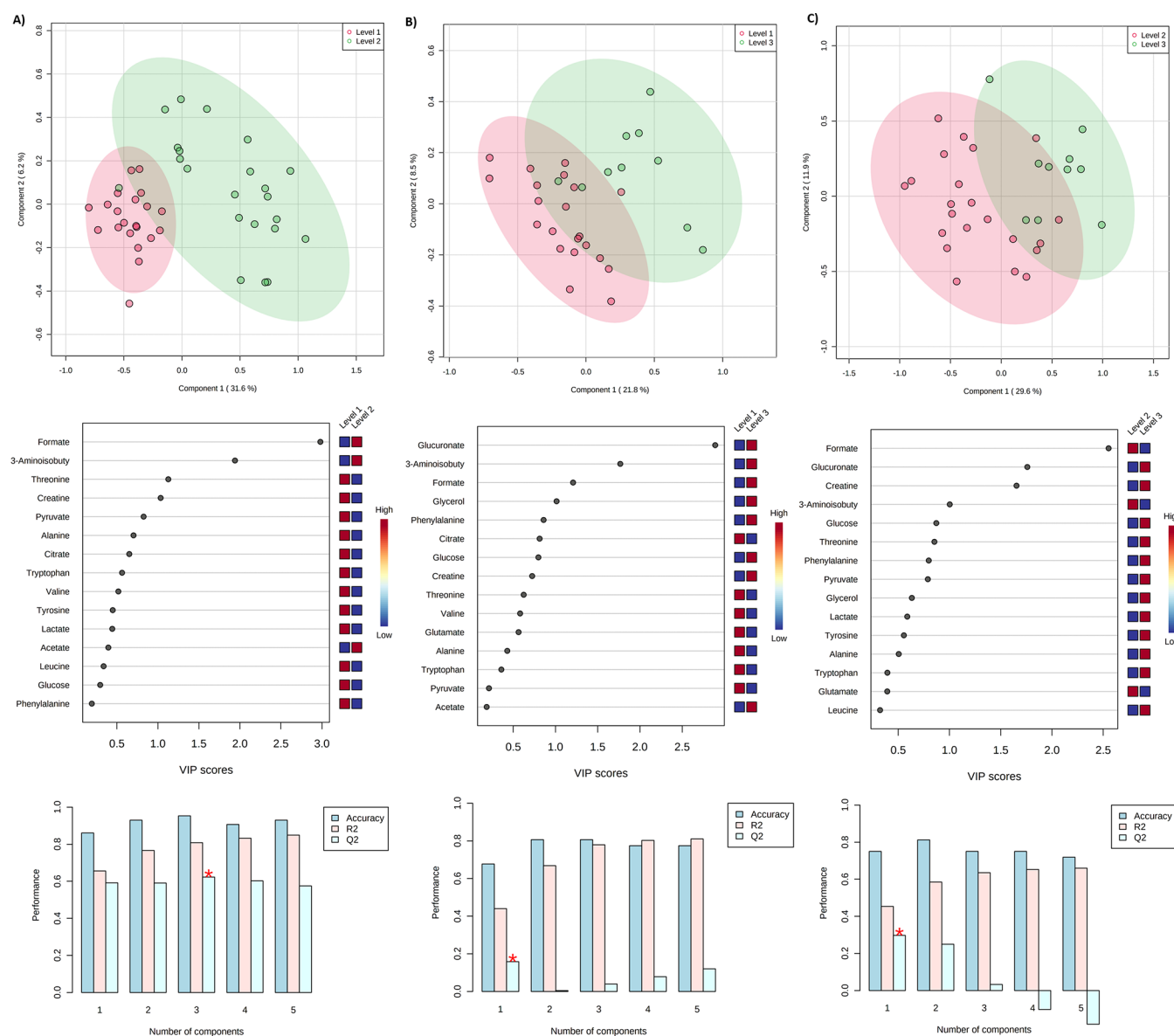


**Figure 3.** PLS-DA, VIP scores, and cross-validation analysis of binary comparisons between Covid-19 subgroups. (A) Level 1 (mild) vs level 2 (moderate) comparison; (B) level 1 (mild) vs level 3 (severe) comparison; and (C) level 2 (moderate) vs level 3 (severe) comparison. ROC curves and probability view from the above comparisons are presented in Figure S5.

with three components, the level 3 group could not be entirely separated from the others (Figure 2B). The PLS-DA cross-validation  $R^2$  and  $Q^2$  coefficients evidenced a moderate classifier model, with values consisting of 0.58 and 0.48, respectively (Figure 2C), and the permutation test, applying the prediction during the training test and 2000 permutations, resulted in an empirical  $p < 0.0005$  (Figure 2D).

Similarly to the previous comparison, glycerol, acetate, and 3-aminoisobutyrate were the most important metabolites for group discrimination, highlighting their relevance in the Covid-19 infection (Figure 2E and Table S2). Glycerol concentration was higher in the control group than in the Covid-19 groups; nevertheless, its concentration in the Covid-19 groups increased accordingly with the severity level. On the other hand, acetate showed an increasing profile for moderate and severe cases (levels 2 and 3), with no statistical difference, although the mean concentration for level 2 was higher. The concentration of 3-aminoisobutyrate was shown to be higher in

the control group and level 2 but with a tendency to decrease for severe cases. The concentration of phenylalanine, glucose, glucuronate, lactate, leucine, and creatine showed a higher concentration for level 3. The metabolite panel, considering binning spectra data, corroborates these results and is shown in Figure S4.

Binary comparisons between the Covid-19 severity level groups were also performed, observing for metabolic differences in each specific condition (Figure 3 and Table S2). PLS-DA models could not separate the groups; however, a clear tendency is shown in each comparison (Figure 3A–C). When considering the univariate data, formate and 3-aminoisobutyrate concentrations, with similarities in control and mild levels, helped differentiate mild from moderate level since their concentration is higher for moderate cases (Figure 3A). On the other hand, glucuronate and 3-aminoisobutyrate concentrations may be used for severe cases distinct from mild cases (Figure 3B), and formate, glucuronate, and creatine concen-

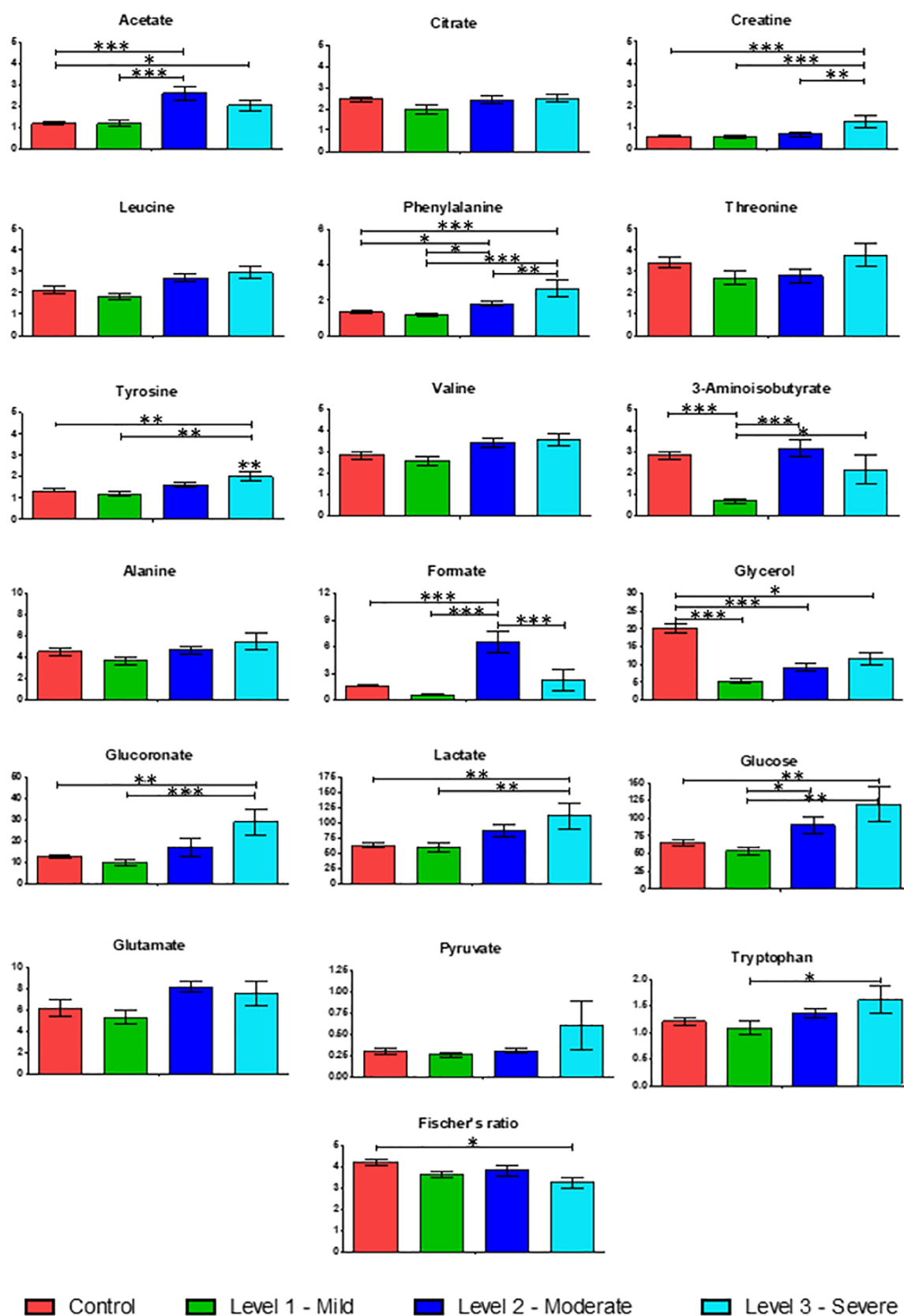


**Figure 4.** Concentration in mg dL<sup>-1</sup> (mean  $\pm$  SEM) of metabolites from blood plasma samples from SARS-CoV-2 virus infection at levels 1–3 patients and healthy individuals that were considered significantly different comparing control versus each level of Covid-19 diseases (see Table S2 for complementary information). Tukey's HSD *p*-value cutoffs were \* *p* < 0.05 (significant), \*\* *p* < 0.01 (very significant), and \*\*\* *p* < 0.001 (highly significant). SEM: standard error of the mean.

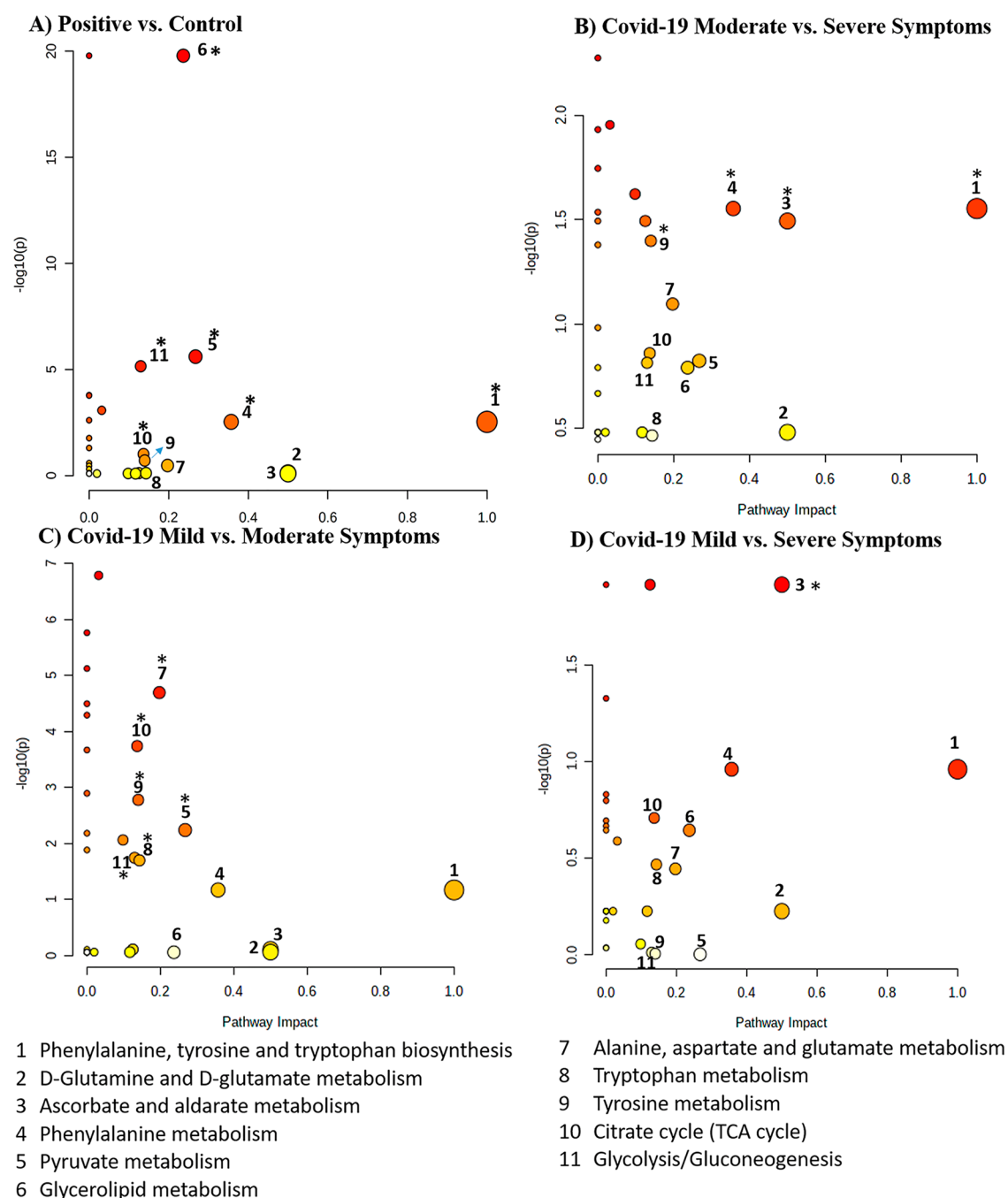


**Figure 5.** Metabolic pathway analysis from different comparisons of Covid-19 samples. (A) Positive *vs* control comparison; (B) level 1 (mild) *vs* level 2 (moderate) comparison; (C) level 1 (mild) *vs* level 3 (severe) comparison; and (D) level 2 (moderate) *vs* level 3 (severe) comparison. The red color indicates the high impact of the respective metabolic pathway (see Tables S3–S6 for complementary information). \*  $p$ -value < 0.05 (significant).

trations can differentiate moderate from severe cases (Figure 3C). Cross-validation of the PLS-DA models showed a good predictive capacity for mild and moderate separation,<sup>30</sup> with a  $Q^2$  of approximately 0.59; however, for mild and severe group's separation, the model showed little predictive relevancy, with a  $Q^2$  of approximately 0.16, and for moderate and severe group's separation, the predictive relevancy was moderate, with a  $Q^2$  approximately 0.3. Results considering binning spectra data corroborate these results and are shown in Figure S6.

The one-way ANOVA analysis showed that 10 of the 18 metabolites were significantly different when comparing control versus each of the severity level groups (Table S2).

However, the one-way ANOVA analysis showed that 11 of the 18 metabolites were significantly different between the severity level groups (Figure 4). The boxplots of each of the 18 metabolite concentrations, in  $\text{mg dL}^{-1}$ , are presented in Figure 4. Supporting the previous PLS-DA multivariate analysis, the glycerol concentration was lower in Covid-19 samples, while lactate concentration increases accordingly with the severity. Phenylalanine, tyrosine, leucine, valine, and creatine concentrations increase along with the increase in severity. Except for leucine and valine, a significant statistical difference was observed ( $p < 0.05$ ) when comparing the control group with severe cases. If phenylalanine and tyrosine concentrations



increase, Fisher's ratio decreases with the severity of Covid-19 cases.

In summary, six metabolites were found to be relevant to discriminating the disease. Glycerol, 3-aminoisobutyrate, and acetate were the three biomarkers to differentiate positive against negative diagnostic of Covid-19, and these metabolites together with formate, glucuronate, and lactate differentiate level 3 against levels 1 and 2, as confirmed by the ROC curve-based model evaluation including metabolite ratios (Figure S7).

### Metabolic Pathway Impact of Covid-19

The individual metabolite concentrations highlighted in the previous comparisons were submitted to metabolic pathway analysis in the MetaboAnalyst platform, revealing alterations in 11 metabolic pathways (Figure 5 and Tables S3–S6). The most impacted pathways were (1–3) phenylalanine, tyrosine, and tryptophan biosynthesis; (4) phenylalanine metabolism; (5) pyruvate metabolism; (6) glycerolipid metabolism; (10) citrate cycle (TCA cycle); and (11) glycolysis/gluconeogenesis. Notwithstanding, the ascorbate and aldarate metabolism pathway does not show  $p$ -value < 0.05 in the control vs Covid-19 sample comparison (Figure 5); these metabolic pathways are relevant in the Covid-19 severity level comparison.

## DISCUSSION

The first creative aspect in this paper regards the analysis of blood plasma sample extracts by  $^1\text{H}$  NMR. Since plasma is a complex matrix rich in proteins, applying a diffusion-edited pulse sequence like Carr–Purcell–Meiboom–Gill (CPMG) for the NMR analysis is typically necessary, suppressing the protein signals and allowing the analysis of small molecules without matrix interference. However, this approach commonly causes a broadening of the baseline, complicating posterior quantitative data analysis. Additionally, the common reference standards used in NMR analysis, such as DSS- $D_6$ , TMSP- $D_4$ , and TSP- $D_4$ , could lead to untrustful quantification data once it has been observed that these standards may bind to proteins and other macromolecules unambiguous in biological fluids.<sup>31</sup> Alternatives to avoid this problem are the use of the proprietary Bruker in vitro diagnostics research (IVDr) method for the entire plasma sample<sup>31</sup> or physically removing proteins and macromolecules from the sample.<sup>26,32</sup> To circumvent this problem, the physical removal of protein by precipitation with cold methanol followed by centrifugation was shown to be an effective alternative for sample preparation, assuring the quality of the quantitative  $^1\text{H}$  NMR data. A positive perspective of our protocol is that, beyond the determination of free (unbound) metabolite concentration in the plasma sample, it also measured the liberated metabolites previously bound to proteins.<sup>31</sup>

Considering that one of the sample preparation steps includes the supernatant drying followed by resolubilization in phosphate buffer and filtration, in this approach, only polar metabolites were extracted, leaving proteins and lipids out of the analysis. Compared with standard protocols using the CPMG pulse sequence and direct analysis of plasma, our results showed more specific information since it leads only to low-molecular-weight molecules to be detected and identified. The protocol also assures the integrity of the metabolites since it avoids possible degradation.<sup>32,33</sup> In addition, our protocol can be considered safer for the analysis of high-risk samples

since the pathogen is inactivated prior to further manipulation, lowering the risk of contamination.<sup>34</sup>

The presence of IgM in most samples confirmed that the volunteers of this study were admitted to the hospital during the early stage of the disease and that sampling protocol was essential to guarantee that patients were not under pharmacological treatments, leading to metabolic changes and misinterpretation of the data.

Data analysis was performed in two main approaches, each designed to answer a specific question. The first approach was the comparison of healthy control plasma samples with Covid-19 patients' samples, regardless of symptom severity. This approach leads to a panel of metabolites as potential biomarkers of Covid-19 infection and shows the most affected metabolic pathways during the disease. Our model generated from this comparison was shown to be highly effective, with only 8 prediction errors out of 110 samples in the confusion matrix and an AUC of 0.924 in the ROC curve, as shown in Figure 1. The second approach compares healthy control samples with Covid-19 symptom severity subgroups, which leads to a metabolite panel for Covid-19 prognosis. In that analysis, besides presenting a moderate predictive coefficient, the PLS-DA model could not entirely separate the level 3 subgroup (severe symptoms) from the remaining subgroups (Figure 2). Notwithstanding, PLS-DA models constructed to binary comparisons between the Covid-19 subgroups showed a moderate separation between mild and moderate levels; however, the models could not satisfactorily separate mild from severe and moderate from severe cases (Figure 3) due to the low predictive coefficient values.

Although identifying a panel of metabolites capable of differentiating mild-to-severe-case symptoms is essential, understanding the metabolite profile of mild to moderate groups might be more suitable for clinical intervention.<sup>35,36</sup>

Regardless of the data analysis approach, the metabolites glycerol, acetate, 3-aminoisobutyrate, formate, glucuronate, and lactate were shown to be highly important for the groups' discrimination (Figures 3 and 4), with the formate, glucuronate, and creatine levels being highly expressed for the severe group (level 3). The metabolic pathways suggested were similar for both approaches, with phenylalanine, tyrosine, and tryptophan biosynthesis being the most outstanding pathway (Figure 5).

### Impacted Metabolites and Metabolic Pathways

Over the past years, many studies have been conducted on Covid-19 patient samples, resulting in a broad knowledge of the contamination process and pathways leading to the symptoms. The SARS-CoV-2 virus enters the cells through ACE2 binding, a receptor found mainly in the lung, liver, intestine, and brain cells, and once in the interior of the cells, it starts the process of viral replication. This process triggers the immune system that relocates metabolic resources to start the production of antibodies and cytokines, looking for targeting viral particles and controlling the virus spreading. However, in SARS-CoV-2 virus infection, the release of the cytokines may be exaggerated, disrupting severe inflammations, mainly related to high production of interleukins (ILs), macrophage colony stimulating factors (M-CSFs), granulocyte colony stimulating factors (G-CSFs), and interferons (IFNs).<sup>37–43</sup>

As mentioned, to produce high concentrations of such proteins, the metabolism needs to adapt and relocate its resources, culminating in a metabolite concentration shift. An

example is the glucose and lipid metabolism, which is known to be shifted during a high production of cytokines TNF- $\alpha$ , IL-6, and IL-1 $\beta$  and during the entry, replication, and egress of the virus at/from the host cell.<sup>42,44–46</sup> In detail, glucose resistance is highlighted during the production of cytokines, while lipolysis and triglyceride synthesis are upregulated. Similarly, it is also known that viruses might alter the host cell metabolism on behalf of its replication, similar to the Warburg effect, widely studied in cancer models, also known as aerobic glycolysis.<sup>47,48</sup> Compared to cancer cells, the virus's replication is highly dependent on the availability of glucose and glutamine (carbon sources) and the tricarboxylic acid cycle (TCA) process. However, viruses reprogram the host cell and control those metabolic pathways and substrates. Each type of virus might control them in a particular manner, and this matter has not been clarified yet.<sup>49,50</sup> Regarding the Covid-19 disease, this information endorses why diabetic patients present higher chances of complication than healthy individuals since their condition enables high cytokine production and high energy support for viral proliferation, aggravating their clinical status.<sup>51,52</sup> Additionally, obese patients with high triglyceride levels support the high production of cytokines and, therefore, the cytokine storm, resulting in more severe cases as well.<sup>48</sup> As per the literature,<sup>53–56</sup> our metabolomics data indicate glycerol as a vital metabolite for group discrimination, and its levels in Covid-19 symptom subgroups increase along with symptom intensity (Figures 1–3). Glycerol is one of the key metabolites for triglyceride production and one of the significant products in lipolysis. Our data show that glucose is elevated in patients under SARS-CoV-2 virus infection, and its levels are higher in the severe symptom group.<sup>57</sup>

In summary, the body's energy metabolism has been altered in Covid-19 patients by observing increased blood glucose and decreased 3-aminobutyrate, implying a lowered glucose use.<sup>58</sup> Together with glucose, other metabolites are presented as crucial to the description of the disease. Bruzzone et al. showed an elevation of 68, 33, 67, and 81% in amounts of glucose, glutamate, pyruvate, and phenylalanine, respectively, in the serum of Covid-19 patients.<sup>53,59,60</sup> In our work, an elevation of 83, 22, 100, and 100%, respectively, is observed for these metabolites in Covid-19 patients comprising the severe level of infection compared with healthy individuals. These data suggest an association between dysregulation of hepatic capacity to oxidize acetyl-CoA in the mitochondria and a general metabolic stress condition in Covid-19 patients.<sup>53</sup> These data can also be corroborated by the increased level of lactate in the severe symptom group and higher formate levels for the moderate symptom group.<sup>59,60</sup>

During the TCA cycle under Warburg conditions (aerobic), the pyruvate is converted to lactate and eliminated from the cells, which might explain its increased concentration (Figure 4).<sup>44,45</sup> Some researchers have been evaluating the use of lactate levels as a guide in risk stratification since the blood levels are significantly different compared to ambulatory versus hospitalized patients, which can be elevated up to 120%.<sup>61</sup> Another study involving 2860 Covid-19 patients related high serum lactate levels to the need for intensive care units (ICUs) and mortality, with patients reaching 150% of increasing lactate levels compared to normal levels.<sup>62</sup> Our data showed 76% elevated lactate levels in the severe patient's group. However, it is worth mentioning that our samples were collected earlier to

the individual's hospitalization, i.e., the first search for help in the medical care system.

Another interesting metabolite highlighted in our data analysis was creatine, which was an important variable for the moderate–severe symptom group separation. Different researchers have evaluated the association between severe Covid-19 infection and creatine kinase (CK), an enzyme in muscle cells responsible for reversibly converting creatine to phosphocreatine.<sup>63–66</sup> Creatine kinase is a known marker for muscular tissue damage since its release in the bloodstream denotes muscular cell breakdown.<sup>67</sup> In severe Covid-19 patients, pneumonia and pulmonary tissue damage are key symptoms; therefore, CK levels are elevated. Phosphocreatine stores energy with higher efficiency than ATP; thus, the conversion of phosphocreatine into creatine enables fast energy release for the muscle cells, supporting its energy requirements.<sup>68</sup> Consequently, in infected lung cells, creatine and phosphocreatine play a significant role in energy supplies, and high creatine levels imply high energy consumption, possibly employed in viral replication.

Besides the roles of specific metabolites, the results of PLS-DA and ANOVA statistical analysis (Figures 1–4) highlight the importance of the pathways: phenylalanine, tyrosine, and tryptophan biosynthesis; phenylalanine metabolism; and pyruvate metabolism. Previous publications on Covid-19 metabolomics support our findings once phenylalanine- and pyruvate-related metabolic pathways are described to be altered in different cohorts.<sup>40,55,58,59,69–71</sup> As discussed above, energy-related metabolic pathways, such as pyruvate metabolism, were shown to be relevant markers for symptom severity due to their close relation with viral replication and cytokine production.

Phenylalanine is an essential amino acid that plays a vital role in the synthesis of proteins and cell proliferation, besides being an energy provider. If hydroxylated, phase-I metabolism is transformed to tyrosine in the liver and then converted to fumarate or acetoacetate. When transported to the brain, this amino acid is converted to L-DOPA, dopamine, epinephrine, and norepinephrine, playing an important neurofunction. According to Figure 4, phenylalanine levels in severe patients are higher, and similar behavior is observed for tyrosine but in slightly lower concentrations. In general, high levels of phenylalanine in plasma mean lower levels of tyrosine and indicate a disturbance in the immune system due to the inducement of apoptosis in human B-cell lines, favoring viral infection and also enabling the attack of opportunistic pathogens.<sup>72–74</sup>

Nevertheless, as discussed in previous paragraphs, our results corroborate with the literature and evidence a panel of metabolites relevant for Covid-19 severity prognosis; however, it is important to discuss the limitations of this study. Our first limitation is the relatively small sample size, particularly for the severe symptom group, which was limited due to our exclusion criteria regarding the patient's previous treatment before the collection of the blood sample. Second, we decided to include patients of different ages in the groups due to the known association between Covid-19 severity and older age. Our rationale was to verify if metabolites related to aging are also correlated with Covid-19 symptoms. Besides that some metabolites highlighted in our panel have been reported as aging markers, such as phenylalanine, lactate, and tyrosine, other aging-related metabolites did not show to be relevant in our data analysis as prognosis markers for Covid-19 severity,

which was the case of valine, leucine, alanine, and glutamate.<sup>75,76</sup> Therefore, our data analysis suggests that metabolic markers of aging cannot be steadily used as markers for severity prognosis, and further studies must be conducted to fully evaluate this hypothesis. Lastly, we have no access to the detailed clinical history of the patients, and possible coexisting conditions may be confounding factors in our data analysis.

Therefore, our data suggest a metabolic shift, particularly in energy and lipid metabolism, to support cytokine production, leading to the cytokine storm, and support the viral replication, leading to an increase in the viral load in the organism. Our data analysis shows that such metabolic shifts are closely related not only to Covid-19 infection but also to the increase in symptom severity. Glycerol, acetate, 3-aminoisobutyrate, formate, glucuronate, and lactate concentrations are potential metabolite candidates for patients' prognosis and may be used in the clinical settings; however, considering the study limitations, further analysis must be carried out in larger cohorts for a panel of metabolite validation and for a comprehensive analysis.

## ■ ASSOCIATED CONTENT

### SI Supporting Information

The Supporting Information is available free of charge at <https://pubs.acs.org/doi/10.1021/acs.jproteome.1c00977>.

Figure S1: <sup>1</sup>H NMR spectrum of a protein-precipitated blood plasma sample from a Covid-19 patient (sample P109); Figure S2: HSQC spectrum processed and analyzed by the COLMARm web server; Figure S3: PLS-DA and cross-validation analysis of NMR metabolomics data as binning spectra showing Covid-19 samples vs health control; Figure S4: PLS-DA and cross-validation analysis of NMR metabolomics data as binning spectra accordingly with Covid-19 symptom severity; Figure S5: ROC curves and probability view; Figure S6: PLS-DA and cross-validation analysis of NMR metabolomics data as binning spectra showing binary comparisons between Covid-19 subgroups; Figure S7: ROC curves and probability view of the six potential prognostic metabolites (glycerol, 3-aminoisobutyrate, acetate, formate, glucuronate, and lactate); Table S1: compound information about HSQC spectrum processed and analyzed by the COLMARm web server; Table S2: metabolite's concentration obtained from negative vs different positive cases of Covid-19 by <sup>1</sup>H NMR analysis; Table S3: metabolic pathways highlighted for the metabolomics profile from positive to negative levels of Covid-19 patients; Table S4: metabolic pathways highlighted for the metabolomics profile from moderate to severe levels of Covid-19 patients; Table S5: metabolic pathways highlighted for the metabolomics profile from mild to moderate levels of Covid-19 patients; and Table S6: metabolic pathways highlighted for the metabolomics profile from mild to severe levels of Covid-19 patients (PDF)

## ■ AUTHOR INFORMATION

### Corresponding Author

Daniel R. Cardoso – Instituto de Química de São Carlos, Universidade de São Paulo, São Carlos, SP 13566-590,

Brazil; [orcid.org/0000-0002-3492-3327](https://orcid.org/0000-0002-3492-3327);

Email: [drcardoso@usp.br](mailto:drcardoso@usp.br)

## Authors

Banny S. B. Correia – Instituto de Química de São Carlos, Universidade de São Paulo, São Carlos, SP 13566-590, Brazil

Vinicius G. Ferreira – Instituto de Química de São Carlos, Universidade de São Paulo, São Carlos, SP 13566-590, Brazil; Instituto Nacional de Ciência e Tecnologia de Bioanalítica, INCTBio, Campinas, SP 13083-861, Brazil

Priscila M. F. D. Piagge – Instituto de Química de São Carlos, Universidade de São Paulo, São Carlos, SP 13566-590, Brazil

Mariana B. Almeida – Instituto de Química de São Carlos, Universidade de São Paulo, São Carlos, SP 13566-590, Brazil; Instituto Nacional de Ciência e Tecnologia de Bioanalítica, INCTBio, Campinas, SP 13083-861, Brazil

Nilson A. Assunção – Instituto de Ciências Ambientais, Químicas e Farmacêuticas, Universidade Federal de São Paulo, São Paulo, SP 09972-270, Brazil

Joyce R. S. Raimundo – Faculdade de Medicina do ABC, Santo André, SP 09060-870, Brazil

Fernando L. A. Fonseca – Faculdade de Medicina do ABC, Santo André, SP 09060-870, Brazil; Departamento de Ciências Farmacêuticas, Universidade Federal de São Paulo, Diadema, SP 09972-270, Brazil

Emanuel Carrilho – Instituto de Química de São Carlos, Universidade de São Paulo, São Carlos, SP 13566-590, Brazil; Instituto Nacional de Ciência e Tecnologia de Bioanalítica, INCTBio, Campinas, SP 13083-861, Brazil; [orcid.org/0000-0001-7351-8220](https://orcid.org/0000-0001-7351-8220)

Complete contact information is available at:

<https://pubs.acs.org/10.1021/acs.jproteome.1c00977>

## Author Contributions

All authors contributed to and approved the final manuscript. B.S.B.C. idealized the project, prepared the samples, executed the NMR and data analysis, and wrote the manuscript. V.G.F. and M.B.A. analyzed the data and wrote the manuscript. P.M.F.D.P. prepared the samples, executed the NMR analysis, and wrote the manuscript. N.A.A., J.R.S.R., and F.L.A.F. idealized the project, discussed the data, and wrote the manuscript. E.C. and D.R.C. idealized and supervised the project, applied for the grant, analyzed the data, and wrote the manuscript.

## Notes

The authors declare no competing financial interest.

## ■ ACKNOWLEDGMENTS

The authors acknowledge the financial support from CAPES (Grant no. 88887.504531/2020-00 from notice no. 09/2020), FAPESP (grant nos. 14/50867-3 and 17/01189-0), and CNPq (INCTBio grant no. 465389/2014-7). DRC and EC acknowledge the continued support from CNPq Research Productivity Program (309212/2019-7).

## ■ REFERENCES

(1) Ritchie, H.; Mathieu, E.; Rodés-Guirao, L.; Appel, C.; Giattino, C.; Ortiz-Ospina, E.; Hasell, J.; Macdonald, B.; Beltekian, D.; Roser, M. Coronavirus Pandemic (COVID-19). <https://ourworldindata.org/>



covid-deahttps://ourworldindata.org/coronavirus (accessed Oct 19, 2021).

(2) Covid-10trn What is the economic cost of covid-19?. <https://outline.com/73aekL>.

(3) COVID Research: A Year of Scientific Milestones. *Nature* 2021. <https://doi.org/10.1038/d41586-020-00502-w>.

(4) Jungreis, I.; Sealfon, R.; Kellis, M. SARS-CoV-2 Gene Content and COVID-19 Mutation Impact by Comparing 44 Sarbecovirus Genomes. *Nat. Commun.* **2021**, *12*, No. 2642.

(5) Pan, Y.; Jiang, X.; Yang, L.; Chen, L.; Zeng, X.; Liu, G.; Tang, Y.; Qian, C.; Wang, X.; Cheng, F.; Lin, J.; Wang, X.; Li, Y. SARS-CoV-2-Specific Immune Response in COVID-19 Convalescent Individuals. *Signal Transduction Targeted Ther.* **2021**, *6*, No. 256.

(6) Starr, T. N.; Greaney, A. J.; Addetia, A.; Hannon, W. W.; Choudhary, M. C.; Dingens, A. S.; Li, J. Z.; Bloom, J. D. Prospective Mapping of Viral Mutations That Escape Antibodies Used to Treat COVID-19. *Science* **2021**, *371*, 850–854.

(7) SARS-CoV-2 Variant Classifications and Definitions. <https://www.cdc.gov/coronavirus/2019-ncov/variants/variant-l#Interest>.

(8) Wu, D.; Wu, T.; Liu, Q.; Yang, Z. The SARS-CoV-2 Outbreak: What We Know. *Int. J. Infect. Dis.* **2020**, *94*, 44–48.

(9) Asim, M.; Sathian, B.; Banerjee, I.; Robinson, J. A Contemporary Insight of Metabolomics Approach for COVID-19: Potential for Novel Therapeutic and Diagnostic Targets. *Nepal J. Epidemiol.* **2020**, *10*, 923–927.

(10) Lai, C. C.; Shih, T. P.; Ko, W. C.; Tang, H. J.; Hsueh, P. R. Severe Acute Respiratory Syndrome Coronavirus 2 (SARS-CoV-2) and Coronavirus Disease-2019 (COVID-19): The Epidemic and the Challenges. *Int. J. Antimicrob. Agents* **2020**, *55*, No. 105924.

(11) Mainous, A. G.; Rooks, B. J.; Wu, V.; Orlando, F. A. COVID-19 Post-Acute Sequelae Among Adults: 12 Month Mortality Risk. *Front. Med.* **2021**, *8*, No. 778434.

(12) Rashedi, J.; Poor, B. M.; Asgharzadeh, V.; Pourostadi, M.; Kafil, H. S.; Vegari, A.; Tayebi-Khosroshahi, H.; Asgharzadeh, M. Risk Factors for Covid-19. *Infez. Med.* **2020**, *28*, 469–474.

(13) Wolff, D.; Nee, S.; Hickey, N. S.; Marschollek, M. Risk Factors for Covid-19 Severity and Fatality: A Structured Literature Review. *Infection* **2021**, *49*, 15–28.

(14) Liang, J.; Jin, G.; Liu, T.; Wen, J.; Li, G.; Chen, L.; Wang, W.; Wang, Y.; Liao, W.; Song, J.; Ding, Z.; Chen, X.; Zhang, B. Clinical Characteristics and Risk Factors for Mortality in Cancer Patients with COVID-19. *Front. Med.* **2021**, *15*, 264–274.

(15) Holmes, E.; Wist, J.; Masuda, R.; Lodge, S.; Nitschke, P.; Kimhofer, T.; Loo, R. L.; Begum, S.; Boughton, B.; Yang, R.; Morillon, A. C.; Chin, S. T.; Hall, D.; Ryan, M.; Bong, S. H.; Gay, M.; Edgar, D. W.; Lindon, J. C.; Richards, T.; Yeap, B. B.; Pettersson, S.; Spraul, M.; Schaefer, H.; Lawler, N. G.; Gray, N.; Whiley, L.; Nicholson, J. K. Incomplete Systemic Recovery and Metabolic Phenoreversion in Post-Acute-Phase Nonhospitalized COVID-19 Patients: Implications for Assessment of Post-Acute COVID-19 Syndrome. *J. Proteome Res.* **2021**, *20*, 3315–3329.

(16) Nalbandian, A.; Sehgal, K.; Gupta, A.; Madhavan, M. V.; McGroder, C.; Stevens, J. S.; Cook, J. R.; Nordvig, A. S.; Shalev, D.; Sehrawat, T. S.; Ahluwalia, N.; Bikdeli, B.; Dietz, D.; Der-Nigoghossian, C.; Liyanage-Don, N.; Rosner, G. F.; Bernstein, E. J.; Mohan, S.; Beckley, A. A.; Seres, D. S.; Choueiri, T. K.; Uriel, N.; Ausiello, J. C.; Accili, D.; Freedberg, D. E.; Baldwin, M.; Schwartz, A.; Brodie, D.; Garcia, C. K.; Elkind, M. S. V.; Connors, J. M.; Bilezikian, J. P.; Landry, D. W.; Wan, E. Y. Post-Acute COVID-19 Syndrome. *Nat. Med.* **2021**, *27*, 601–615.

(17) Al-Jahdhami, I.; Al-Namani, K.; Al-Mawali, A. The Post-Acute COVID-19 Syndrome (Long COVID). *Oman Med. J.* **2021**, *36*, e220.

(18) Say, D.; Crawford, N.; McNab, S.; Wurzel, D.; Steer, A.; Tosif, S. Post-Acute COVID-19 Outcomes in Children with Mild and Asymptomatic Disease. *Lancet Child Adolesc. Health* **2021**, *5*, e22–e23.

(19) Xie, Y.; Bowe, B.; Al-Aly, Z. Burdens of Post-Acute Sequelae of COVID-19 by Severity of Acute Infection, Demographics and Health Status. *Nat. Commun.* **2021**, *12*, No. 6571.

(20) Malik, P.; Patel, K.; Pinto, C.; Jaiswal, R.; Tirupathi, R.; Pillai, S.; Patel, U. Post-acute COVID-19 Syndrome (PCS) and Health-related Quality of Life (HRQoL)—A Systematic Review and Meta-analysis. *J. Med. Virol.* **2022**, *94*, 253–262.

(21) Sharma, A.; Tiwari, S.; Kanti, M.; Louis, J. Since January 2020 Elsevier Has Created a COVID-19 Resource Centre with Free Information in English and Mandarin on the Novel Coronavirus COVID-19. The COVID-19 Resource Centre Is Hosted on Elsevier Connect, the Company's Public News and Information. *Science* **2020**, *56*, 1–14.

(22) Yang, X.; Yu, Y.; Xu, J.; Shu, H.; Xia, J.; Liu, H.; Wu, Y.; Zhang, L.; Yu, Z.; Fang, M.; Yu, T.; Wang, Y.; Pan, S.; Zou, X.; Yuan, S.; Shang, Y. Clinical Course and Outcomes of Critically Ill Patients with SARS-CoV-2 Pneumonia in Wuhan, China: A Single-Centered, Retrospective, Observational Study. *Lancet Respir. Med.* **2020**, *8*, 475–481.

(23) Sanchez, E. L.; Lagunoff, M. Viral Activation of Cellular Metabolism. *Virology* **2015**, *479–480*, 609–618.

(24) Wu, D.; Shu, T.; Yang, X.; Song, J. X.; Zhang, M.; Yao, C.; Liu, W.; Huang, M.; Yu, Y.; Yang, Q.; Zhu, T.; Xu, J.; Mu, J.; Wang, Y.; Wang, H.; Tang, T.; Ren, Y.; Wu, Y.; Lin, S. H.; Qiu, Y.; Zhang, D. Y.; Shang, Y.; Zhou, X. Plasma Metabolomic and Lipidomic Alterations Associated with COVID-19. *Natl. Sci. Rev.* **2020**, *7*, 1157–1168.

(25) Emwas, A. H.; Roy, R.; McKay, R. T.; Tenori, L.; Saccenti, E.; Nagana Gowda, G. A.; Raftery, D.; Alahmari, F.; Jaremko, L.; Jaremko, M.; Wishart, D. S. Nmr Spectroscopy for Metabolomics Research. *Metabolites* **2019**, *9*, No. 123.

(26) Nagana Gowda, G. A.; Raftery, D. Analysis of Plasma, Serum, and Whole Blood Metabolites Using 1H NMR Spectroscopy. In *NMR-Based Metabolomics. Methods in Molecular Biology*; Humana: New York, NY, 2019; Vol. 2037, pp 17–34.

(27) Jin, J.-M.; Bai, P.; He, W.; Wu, F.; Liu, X.-F.; Han, D.-M.; Liu, S.; Yang, J.-K. Gender Differences in Patients With COVID-19: Focus on Severity and Mortality. *Front. Public Heal.* **2020**, *8*, No. 152.

(28) Nakanishi, T.; Pigazzini, S.; Degenhardt, F.; Cordioli, M.; Butler-Laporte, G.; Maya-Miles, D.; Bujanda, L.; Bouysran, Y.; Niemi, M. E. K.; Palom, A.; Ellinghaus, D.; Khan, A.; Martínez-Bueno, M.; Rolker, S.; Amitrano, S.; Roade Tato, L.; Fava, F.; Spinner, C. D.; Prati, D.; Bernardo, D.; Garcia, F.; Darcis, G.; Fernández-Cadenas, I.; Holter, J. C.; Banales, J. M.; Frithiof, R.; Kiryluk, K.; Duga, S.; Asselta, R.; Pereira, A. C.; Romero-Gómez, M.; Nafria-Jiménez, B.; Hov, J. R.; Migeotte, I.; Renieri, A.; Planas, A. M.; Ludwig, K. U.; Buti, M.; Rahmouni, S.; Alarcón-Riquelme, M. E.; Schulte, E. C.; Franke, A.; Karlsen, T. H.; Valenti, L.; Zeberg, H.; Richards, J. B.; Ganna, A. Age-Dependent Impact of the Major Common Genetic Risk Factor for COVID-19 on Severity and Mortality. *J. Clin. Invest.* **2021**, *131*, No. e152386.

(29) Williamson, E. J.; Walker, A. J.; Bhaskaran, K.; Bacon, S.; Bates, C.; Morton, C. E.; Curtis, H. J.; Mehrkar, A.; Evans, D.; Inglesby, P.; Cockburn, J.; McDonald, H. I.; MacKenna, B.; Tomlinson, L.; Douglas, I. J.; Rentsch, C. T.; Mathur, R.; Wong, A. Y. S.; Grieve, R.; Harrison, D.; Forbes, H.; Schultze, A.; Croker, R.; Parry, J.; Hester, F.; Harper, S.; Perera, R.; Evans, S. J. W.; Smeeth, L.; Goldacre, B. Factors Associated with COVID-19-Related Death Using OpenSAFELY. *Nature* **2020**, *584*, 430–436.

(30) Hair, J. F.; Risher, J. J.; Sarstedt, M.; Ringle, C. M. When to Use and How to Report the Results of PLS-SEM. *Eur. Bus. Rev.* **2019**, *31*, 2–24.

(31) Crook, A. A.; Powers, R. Quantitative NMR-Based Biomedical Metabolomics: Current Status and Applications. *Molecules* **2020**, *25*, No. 5128.

(32) Loo, R. L.; Lodge, S.; Kimhofer, T.; Bong, S. H.; Begum, S.; Whiley, L.; Gray, N.; Lindon, J. C.; Nitschke, P.; Lawler, N. G.; Schäfer, H.; Spraul, M.; Richards, T.; Nicholson, J. K.; Holmes, E. Quantitative In-Vitro Diagnostic NMR Spectroscopy for Lipoprotein and Metabolite Measurements in Plasma and Serum: Recommendations for Analytical Artifact Minimization with Special Reference to COVID-19/SARS-CoV-2 Samples. *J. Proteome Res.* **2020**, *19*, 4428–4441.

- (33) Snytnikova, O. A.; Khlichkina, A. A.; Sagdeev, R. Z.; Tsentulovich, Y. P. Evaluation of Sample Preparation Protocols for Quantitative NMR-Based Metabolomics. *Metabolomics* **2019**, *15*, No. 84.
- (34) Patterson, E. I.; Prince, T.; Anderson, E. R.; Casas-Sanchez, A.; Smith, S. L.; Cansado-Utrilla, C.; Solomon, T.; Griffiths, M. J.; Acosta-Serrano, A.; Turtle, L.; Hughes, G. L. Methods of Inactivation of SARS-CoV-2 for Downstream Biological Assays. *J. Infect. Dis.* **2020**, *222*, 1462–1467.
- (35) Song, J. W.; Zhang, C.; Fan, X.; Meng, F. P.; Xu, Z.; Xia, P.; Cao, W. J.; Yang, T.; Dai, X. P.; Wang, S. Y.; Xu, R. N.; Jiang, T. J.; Li, W. G.; Zhang, D. W.; Zhao, P.; Shi, M.; Agrati, C.; Ippolito, G.; Maeurer, M.; Zumla, A.; Wang, F. S.; Zhang, J. Y. Immunological and Inflammatory Profiles in Mild and Severe Cases of COVID-19. *Nat. Commun.* **2020**, *11*, No. 3410.
- (36) Zhai, W.; Luo, Z.; Zheng, Y.; Dong, D.; Wu, E.; Wang, Z.; Zhai, J.; Han, Y.; Liu, H.; Wang, Y.; Feng, Y.; Wang, J.; Ma, Y. Moderate vs. Mild Cases of Overseas-Imported COVID-19 in Beijing: A Retrospective Cohort Study. *Sci. Rep.* **2021**, *11*, No. 6483.
- (37) Shang, J.; Wan, Y.; Luo, C.; Ye, G.; Geng, Q.; Auerbach, A.; Li, F. Cell Entry Mechanisms of SARS-CoV-2. *Proc. Natl. Acad. Sci. U.S.A.* **2020**, *117*, 11727–11734.
- (38) Hoffmann, M.; Kleine-Weber, H.; Schroeder, S.; Krüger, N.; Herrler, T.; Erichsen, S.; Schiergens, T. S.; Herrler, G.; Wu, N. H.; Nitsche, A.; Müller, M. A.; Drosten, C.; Pöhlmann, S. SARS-CoV-2 Cell Entry Depends on ACE2 and TMPRSS2 and Is Blocked by a Clinically Proven Protease Inhibitor. *Cell* **2020**, *181*, 271–280.e8.
- (39) Letko, M.; Marzi, A.; Munster, V. Functional Assessment of Cell Entry and Receptor Usage for SARS-CoV-2 and Other Lineage B Betacoronaviruses. *Nat. Microbiol.* **2020**, *5*, 562–569.
- (40) Doğan, H. O.; Şenol, O.; Bolat, S.; Yıldız, Ş.N.; Büyüktuna, S. A.; Sartısmailoğlu, R.; Doğan, K.; Hasbek, M.; Hekim, S. N. Understanding the Pathophysiological Changes via Untargeted Metabolomics in COVID-19 Patients. *J. Med. Virol.* **2021**, *93*, 2340–2349.
- (41) González Plaza, J. J.; Hulak, N.; Kausova, G.; Zhumadilov, Z.; Akilzhanova, A. Role of Metabolism during Viral Infections, and Crosstalk with the Innate Immune System. *Intractable Rare Dis. Res.* **2016**, *5*, 90–96.
- (42) Bodhale, N.; Ohms, M.; Ferreira, C.; Mesquita, I.; Mukherjee, A.; André, S.; Sarkar, A.; Estaquier, J.; Laskay, T.; Saha, B.; Silvestre, R. Cytokines and Metabolic Regulation: A Framework of Bidirectional Influences Affecting Leishmania Infection. *Cytokine* **2021**, *147*, No. 155267.
- (43) Costela-ruiz, V. J.; Illescas-montes, R.; Puerta-puerta, J. M.; Ruiz, C.; Melguizo-rodríguez, L. Since January 2020 Elsevier Has Created a COVID-19 Resource Centre with Free Information in English and Mandarin on the Novel Coronavirus COVID-19. The COVID-19 Resource Centre Is Hosted on Elsevier Connect, the Company's Public News and Information. 2020, No. January.
- (44) Sánchez-García, F. J.; Pérez-Hernández, C. A.; Rodríguez-Murillo, M.; Moreno-Altamirano, M. M. B. The Role of Tricarboxylic Acid Cycle Metabolites in Viral Infections. *Front. Cell. Infect. Microbiol.* **2021**, *11*, No. 725043.
- (45) Mayer, K. A.; Stöckl, J.; Zlabinger, G. J.; Gualdoni, G. A. Hijacking the Supplies: Metabolism as a Novel Facet of Virus-Host Interaction. *Front. Immunol.* **2019**, *10*, No. 1533.
- (46) Shi, J.; Fan, J.; Su, Q.; Yang, Z. Cytokines and Abnormal Glucose and Lipid Metabolism. *Front. Endocrinol.* **2019**, *10*, No. 703.
- (47) Warburg, O. On the Origin of Cancer Cells. *Science* **1956**, *123*, 309–314.
- (48) DeBerardinis, R. J.; Chandel, N. S. We Need to Talk about the Warburg Effect. *Nat. Metab.* **2020**, *2*, 127–129.
- (49) Prusinkiewicz, M. A.; Mymryk, J. S. Metabolic Reprogramming of the Host Cell by Human Adenovirus Infection. *Viruses* **2019**, *11*, No. 141.
- (50) Icard, P.; Lincet, H.; Wu, Z.; Coquerel, A.; Forgez, P.; Alifano, M.; Fournel, L. The Key Role of Warburg Effect in SARS-CoV-2 Replication and Associated Inflammatory Response. *Biochimie* **2021**, *180*, 169–177.
- (51) Smith, S. M.; Boppana, A.; Traupman, J. A.; Unson, E.; Maddock, D. A.; Chao, K.; Dobesh, D. P.; Brufsky, A.; Connor, R. I. Impaired Glucose Metabolism in Patients with Diabetes, Prediabetes, and Obesity Is Associated with Severe COVID-19. *J. Med. Virol.* **2021**, *93*, 409–415.
- (52) Mahrooz, A.; Muscogiuri, G.; Buzzetti, R.; Maddaloni, E. The Complex Combination of COVID-19 and Diabetes: Pleiotropic Changes in Glucose Metabolism. *Endocrine* **2021**, *72*, 317–325.
- (53) Bruzzzone, C.; Bizkarguenaga, M.; Gil-Redondo, R.; Diercks, T.; Arana, E.; García de Vicuña, A.; Seco, M.; Bosch, A.; Palazón, A.; San Juan, I.; Laín, A.; Gil-Martínez, J.; Bernardo-Seisdedos, G.; Fernández-Ramos, D.; Lopitz-Otsoa, F.; Embade, N.; Lu, S.; Mato, J. M.; Millet, O. SARS-CoV-2 Infection Dysregulates the Metabolomic and Lipidomic Profiles of Serum. *iScience* **2020**, *23*, No. 101645.
- (54) Blasco, H.; Bessy, C.; Plantier, L.; Lefevre, A.; Piver, E.; Bernard, L.; Marlet, J.; Stefic, K.; Benz-de Bretagne, I.; Cannet, P.; Lumbu, H.; Morel, T.; Boulard, P.; Andres, C. R.; Vourc'h, P.; Héroult, O.; Guillon, A.; Emond, P. The Specific Metabolome Profiling of Patients Infected by SARS-CoV-2 Supports the Key Role of Tryptophan-Nicotinamide Pathway and Cytosine Metabolism. *Sci. Rep.* **2020**, *10*, No. 16824.
- (55) Barberis, E.; Amede, E.; Tavecchia, M.; Marengo, E.; Cittone, M. G.; Rizzi, E.; Pedrinelli, A. R.; Tonello, S.; Minisini, R.; Piri, M.; Manfredi, M.; Sainaghi, P. P. Understanding Protection from SARS-CoV-2 Using Metabolomics. *Sci. Rep.* **2021**, *11*, No. 13796.
- (56) Pang, Z.; Zhou, G.; Chong, J.; Xia, J. Comprehensive Meta-Analysis of Covid-19 Global Metabolomics Datasets. *Metabolites* **2021**, *11*, No. 44.
- (57) Xue, L. L.; Chen, H. H.; Jiang, J. G. Implications of Glycerol Metabolism for Lipid Production. *Prog. Lipid Res.* **2017**, *68*, 12–25.
- (58) Baranovicova, E.; Bobcakova, A.; Vysehradsky, R.; Dankova, Z.; Halasova, E.; Nosal, V.; Lehotsky, J. The Ability to Normalise Energy Metabolism in Advanced Covid-19 Disease Seems to Be One of the Key Factors Determining the Disease Progression—a Metabolomic Nmr Study on Blood Plasma. *Appl. Sci.* **2021**, *11*, No. 4231.
- (59) Masuda, R.; Lodge, S.; Nitschke, P.; Spraul, M.; Schaefer, H.; Bong, S. H.; Kimhofer, T.; Hall, D.; Loo, R. L.; Bizkarguenaga, M.; Bruzzzone, C.; Gil-Redondo, R.; Embade, N.; Mato, J. M.; Holmes, E.; Wist, J.; Millet, O.; Nicholson, J. K. Integrative Modeling of Plasma Metabolic and Lipoprotein Biomarkers of SARS-CoV-2 Infection in Spanish and Australian COVID-19 Patient Cohorts. *J. Proteome Res.* **2021**, *20*, 4139–4152.
- (60) Lodge, S.; Nitschke, P.; Kimhofer, T.; Coudert, J. D.; Begum, S.; Bong, S. H.; Richards, T.; Edgar, D.; Raby, E.; Spraul, M.; Schaefer, H.; Lindon, J. C.; Loo, R. L.; Holmes, E.; Nicholson, J. K. NMR Spectroscopic Windows on the Systemic Effects of SARS-CoV-2 Infection on Plasma Lipoproteins and Metabolites in Relation to Circulating Cytokines. *J. Proteome Res.* **2021**, *20*, 1382–1396.
- (61) Velavan, T. P.; Linh, L. T. K.; Kreidenweiss, A.; Gabor, J.; Krishna, S.; Kremsner, P. G. Longitudinal Monitoring of Lactate in Hospitalized and Ambulatory COVID-19 Patients. *Am. J. Trop. Med. Hyg.* **2021**, *104*, 1041–1044.
- (62) Bruno, R. R.; Wernly, B.; Flaatten, H.; Fjølner, J.; Artigas, A.; Bollen Pinto, B.; Schefold, J. C.; Binnebössel, S.; Baldia, P. H.; Kelm, M.; Beil, M.; Sigal, S.; van Heerden, P. V.; Szczeklik, W.; Elhadi, M.; Joannidis, M.; Oeyen, S.; Zafeiridis, T.; Wollborn, J.; Arche Banzo, M. J.; Fuest, K.; Marsh, B.; Andersen, F. H.; Moreno, R.; Leaver, S.; Boumendil, A.; De Lange, D. W.; Guidet, B.; Jung, C. COVIP Study Group. Lactate Is Associated with Mortality in Very Old Intensive Care Patients Suffering from COVID-19: Results from an International Observational Study of 2860 Patients. *Ann. Intensive Care* **2021**, *11*, 128.
- (63) Orsucci, D.; Trezzi, M.; Anichini, R.; Blanc, P.; Barontini, L.; Biagini, C.; Capitanini, A.; Comoglio, M.; Corsini, P.; Gemignani, F.; Giannecchini, R.; Giusti, M.; Lombardi, M.; Marrucci, E.; Natali, A.; Nenci, G.; Vannucci, F.; Volpi, G. Increased Creatine Kinase May Predict a Worse Covid-19 Outcome. *J. Clin. Med.* **2021**, *10*, No. 1734.



(64) Orsucci, D. Is Creatine Kinase Associated with Outcome in COVID-19? *Neuroimmunol. Neuroinflammation* **2020**, *2020*, 216–221.

(65) Ji, T.; Liu, Z.; Wang, G. Q.; Guo, X.; Akbar khan, S.; Lai, C.; Chen, H.; Huang, S.; Xia, S.; Chen, B.; Jia, H.; Chen, Y.; Zhou, Q. Detection of COVID-19: A Review of the Current Literature and Future Perspectives. *Biosens. Bioelectron.* **2020**, *166*, No. 112455.

(66) Akbar, M. R.; Pranata, R.; Wibowo, A.; Lim, M. A.; Sihite, T. A.; Martha, J. W. The Prognostic Value of Elevated Creatine Kinase to Predict Poor Outcome in Patients with COVID-19 - A Systematic Review and Meta-Analysis. *Diabetes Metab. Syndr. Clin. Res. Rev.* **2021**, *15*, 529–534.

(67) Clarkson, P. M.; Kearns, A. K.; Rouzier, P.; Rubin, R.; Thompson, P. D. Serum Creatine Kinase Levels and Renal Function Measures in Exertional Muscle Damage. *Med. Sci. Sports Exerc.* **2006**, *38*, 623–627.

(68) Wallimann, T.; Tokarska-Schlattner, M.; Schlattner, U. The Creatine Kinase System and Pleiotropic Effects of Creatine. *Amino Acids* **2011**, *40*, 1271–1296.

(69) Beale, D. J.; Shah, R.; Karpe, A. V.; Hillyer, K. E.; McAuley, A. J.; Au, G. G.; Marsh, G. A.; Vasan, S. S. Metabolic Profiling from an Asymptomatic Ferret Model of Sars-Cov-2 Infection. *Metabolites* **2021**, *11*, No. 327.

(70) Páez-Franco, J. C.; Torres-Ruiz, J.; Sosa-Hernández, V. A.; Cervantes-Díaz, R.; Romero-Ramírez, S.; Pérez-Fragoso, A.; Meza-Sánchez, D. E.; Germán-Acacio, J. M.; Maravillas-Montero, J. L.; Mejía-Domínguez, N. R.; Ponce-de-León, A.; Ulloa-Aguirre, A.; Gómez-Martín, D.; Llorente, L. Metabolomics Analysis Reveals a Modified Amino Acid Metabolism That Correlates with Altered Oxygen Homeostasis in COVID-19 Patients. *Sci. Rep.* **2021**, *11*, No. 6350.

(71) Sindelar, M.; Stancliffe, E.; Schwaiger-Haber, M.; Anbukumar, D. S.; Adkins-Travis, K.; Goss, C. W.; O'Halloran, J. A.; Mudd, P. A.; Liu, W. C.; Albrecht, R. A.; García-Sastre, A.; Shriver, L. P.; Patti, G. J. Longitudinal Metabolomics of Human Plasma Reveals Prognostic Markers of COVID-19 Disease Severity. *Cell Reports Med.* **2021**, *2*, No. 100369.

(72) Sadeghi, M.; Lahdou, I.; Daniel, V.; Schnitzler, P.; Fusch, G.; Schefold, J. C.; Zeier, M.; Iancu, M.; Opelz, G.; Terness, P. Strong Association of Phenylalanine and Tryptophan Metabolites with Activated Cytomegalovirus Infection in Kidney Transplant Recipients. *Hum. Immunol.* **2012**, *73*, 186–192.

(73) Geisler, S.; Gostner, J. M.; Becker, K.; Ueberall, F.; Fuchs, D. Immune Activation and Inflammation Increase the Plasma Phenylalanine-to-Tyrosine Ratio. *Pteridines* **2013**, *24*, 27–31.

(74) An, L.; Lin, L.; Wang, S.; Xie, T.; Yang, Y.; Zhai, W.; Du, L.; Li, W.; Shen, C.; Zhang, Y.; Shan, J. Plasma Characteristic Metabolites of Pediatric Community-Acquired Pneumonia in Traditional Chinese Medicine Syndrome Differentiation. *Anat. Rec.* **2021**, *304*, 2579–2591.

(75) Zhang, F.; Kerbl-Knapp, J.; Akhmetshina, A.; Korbelius, M.; Kuentzel, K. B.; Vujić, N.; Hörl, G.; Paar, M.; Kratky, D.; Steyrer, E.; Madl, T. Tissue-Specific Landscape of Metabolic Dysregulation during Ageing. *Biomolecules* **2021**, *11*, No. 235.

(76) Lawton, K. A.; Berger, A.; Mitchell, M.; Milgram, K. E.; Evans, A. M.; Guo, L.; Hanson, R. W.; Kalhan, S. C.; Ryals, J. A.; Milburn, M. V. Analysis of the adult human plasma metabolome. *Pharmacogenomics* **2008**, *9*, 383–397.